

SHORT COMMUNICATIONS

STRESSES FOR AN ELASTIC HALF-SPACE UNIFORMLY INDENTED BY A RIGID RECTANGULAR FOOTING

S. J. MULLAN AND G. B. SINCLAIR

Carnegie-Mellon University, Pittsburgh, Pennsylvania, U.S.A.

AND

P. W. BROTHERS

Department of Scientific and Industrial Research, Lower Hutt, New Zealand

INTRODUCTION

Elastic solutions, while corresponding to an idealized material behaviour not generally found in soils, do, however, furnish useful working estimates in geomechanics. One collection of such solutions for this purpose can be found in Poulos and Davis.¹ The objective of the present note is to add to this library of elastic stress tables those stresses found under a flat-ended rigid rectangular footing which is uniformly pressed into an elastic half-space. Two conditions between the footing and the half-space are treated: a smooth or lubricated condition where there is no resistance to transverse motion under the footing, and a rough condition wherein transverse motion is completely restrained.

Analyses of the smooth rigid rectangular footing can be found in Conway and Farnham,² Gorbunov-Possadov and Serebrjanyi,³ Borodachev and Galin⁴ and an analysis of both the smooth and rough footing in Brothers *et al.*⁵ In Reference 5 a numerical method is developed which is shown to have superior accuracy to the methods used in References 2 to 4. Accordingly we use the results found *via* Reference 5 as a basis for the stress distributions presented here.

We begin with a statement of the problem, then exhibit and discuss the contact stresses. The note concludes with the presentation of stress components in the interior of the half-space and a comparison of these stresses with values for other related problems.

PROBLEM DESCRIPTION

We are concerned with the uniform indentation of an elastic half-space by a rectangular footing (Figure 1). To describe this geometry we introduce rectangular Cartesian coordinates (x, y, z) and let the half-space H and the surface of H , ∂H , be given by

$$H = \{(x, y, z) | -\infty < x < \infty, -\infty < y < \infty, z > 0\}$$

$$\partial H = \{(x, y, z) | -\infty < x < \infty, -\infty < y < \infty, z = 0\}$$

The footing is flat-ended and rectangular in shape with sides $2a$ and $2b$ parallel to the x - and y -axes respectively. Thus if the contact region below the footing is C while the portion of ∂H

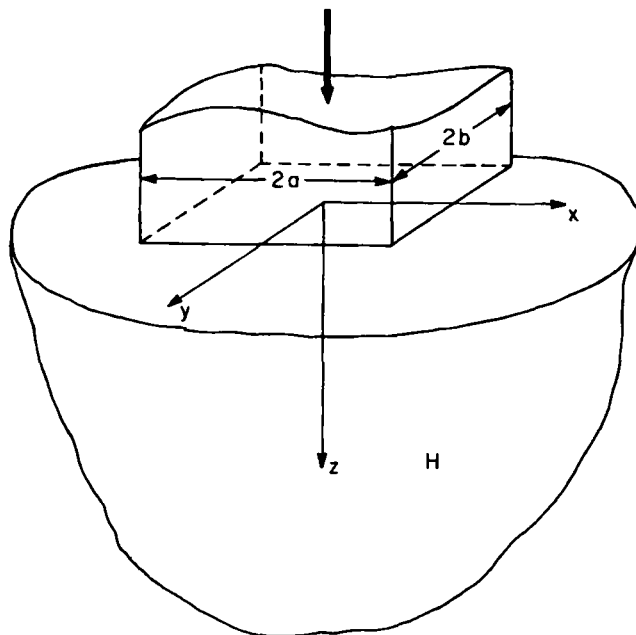


Figure 1. Geometry and coordinate system for the half-space and footing

that is not in contact with the footing is S , we have

$$C = \{(x, y, z) | -a < x < a, -b < y < b, z = 0\}$$

$$S = \{(x, y, z) | a < |x| < \infty, b < |y| < \infty, z = 0\}$$

We seek then the stresses, and in particular the normal stresses $(\sigma_x, \sigma_y, \sigma_z)$, satisfying the field equations throughout H for a linear elastic, homogeneous and isotropic, continuum (Poisson's ratio ν , Young's modulus E) and meeting the boundary conditions on ∂H appropriate to the two cases of a smooth rigid footing and a rough rigid footing, *viz*:

$$w = \delta, \tau_{xz} = \tau_{yz} = 0 \text{ (smooth footing)}$$

$$w = \delta, u = v = 0 \text{ (rough footing)}$$

on C , where u, v and w are the displacements in the x -, y -, and z -directions respectively, δ is the constant depth of penetration of the footing and τ_{xz}, τ_{yz} denote shear stress components in the usual way, together with

$$\sigma_z = \tau_{xz} = \tau_{yz} = 0$$

on S , where σ_z is the normal stress component on a z -face.

CONTACT STRESSES

The analysis of this problem is contained in Reference 5 which also presents results for the surface displacements (in effect, curves of the average normal contact stress, σ_{zav} , *versus* δ for various aspect ratios, α); here we merely give the results for the stresses, beginning with the contact stresses.

The distributions of the normal stress component σ_z are shown in Figures 2 and 3 for both the smooth and rough situations. Quarter-plane symmetry is taken advantage of so that stresses are given for only one quadrant. The dimensionless normal stress component, σ_z/σ_{zav} , is independent of Poisson's ratio for the smooth footing and nearly so for the rough footing, as indicated in

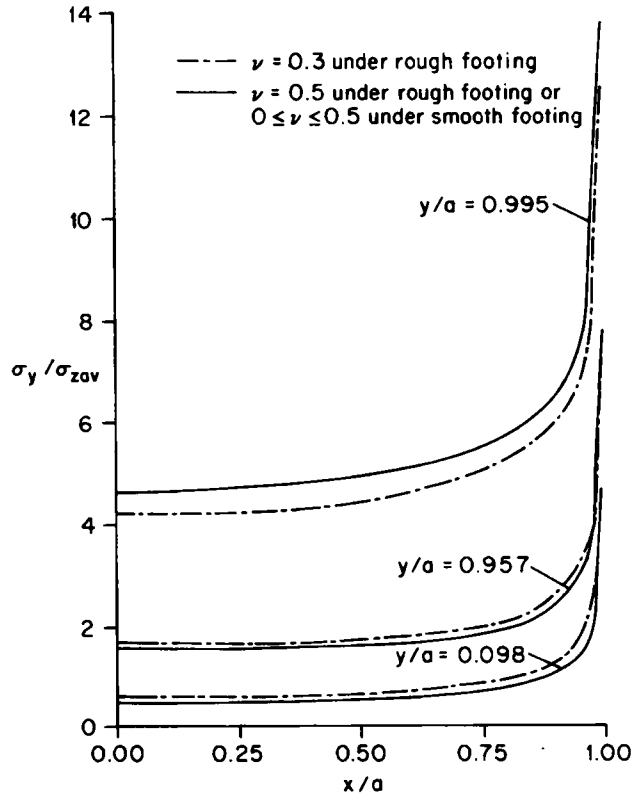


Figure 2. Normal contact stress for rough and smooth square footings

Figure 2 which presents σ_z/σ_{zav} for a square footing (aspect ratio $\alpha = b/a = 1$) for $\nu = 0.3, 0.5$. At $\nu = 0.5$ the results for the rough footing are identical with those for the smooth. Moreover the shear stresses, which are identically zero for the smooth footing, are small in comparison with the normal contact stress for the rough footing (under the footing away from the edges less than 10 per cent of the corresponding normal contact stress). Hence we confine our presentation of results in the remainder of this note to those stemming from the smooth footing—the simpler of the two cases. Figure 3 shows the effect of varying the aspect ratio of the smooth footing ($\alpha = 2, 5$) on the dimensionless normal stress σ_z/σ_{zav} . The contact area of all footings is kept constant regardless of the value of aspect ratio and as a result a varies with α ($a = 1, \alpha = 1$; $a = 0.707, \alpha = 2$; $a = 0.446, \alpha = 5$). As either x/a or y/b approach 1, the results given in Figures 2 and 3 reflect the singular behaviour of the elastic contact stresses beneath a rigid rectangular footing.

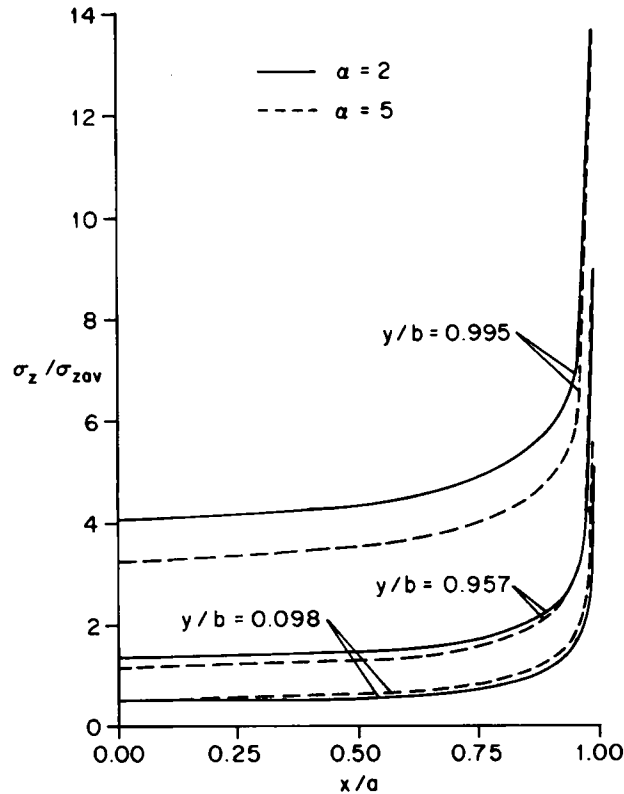


Figure 3. Normal contact stress for a smooth rectangular footing with varying aspect ratio (α)

INTERIOR STRESSES

We next describe the stresses within the interior of the half-space indented by a smooth, rigid, rectangular footing, and compare the results with those for a smooth, rigid, circular footing and a flexible rectangular footing,[†] with all footings sharing a common area. The rigid rectangular stress curves are obtained from the superposition of interior stress response to contact stresses distributed as in Figures 2 and 3 (detailed surface distributions are given in Reference 6). The stresses beneath the rigid circular footing are from Sneddon⁷ and those for the flexible rectangular footing are from Holl.⁸ In order to make these comparisons we use a sequence of four figures which contain the dimensionless stresses, σ/σ_{z0v} , plotted as a function of the dimensionless depth into the half-space, z/a , where σ represents the pertinent normal stress component (σ_x , σ_y , σ_z) and σ_{z0v} is the average normal contact stress.

The first of these, Figure 4, shows the normal stresses in the interior of the half-space along the centroidal axis ($x = y = 0$) under a square ($\alpha = 1$) footing. Here $\sigma_x = \sigma_y$, so that only curves representing stresses on the x - and z -faces are presented. Values are also given for beneath the rigid circular footing ($r = 1.1284a$, where r is the radius) and the flexible square footing. Unlike the contact stress under the smooth rectangular footing, these interior stress components do depend upon Poisson's ratio; however, variations are slight (less than 7 per cent for ν varying

[†] The so-called 'flexible footing' is actually merely a uniform rectangular loading.

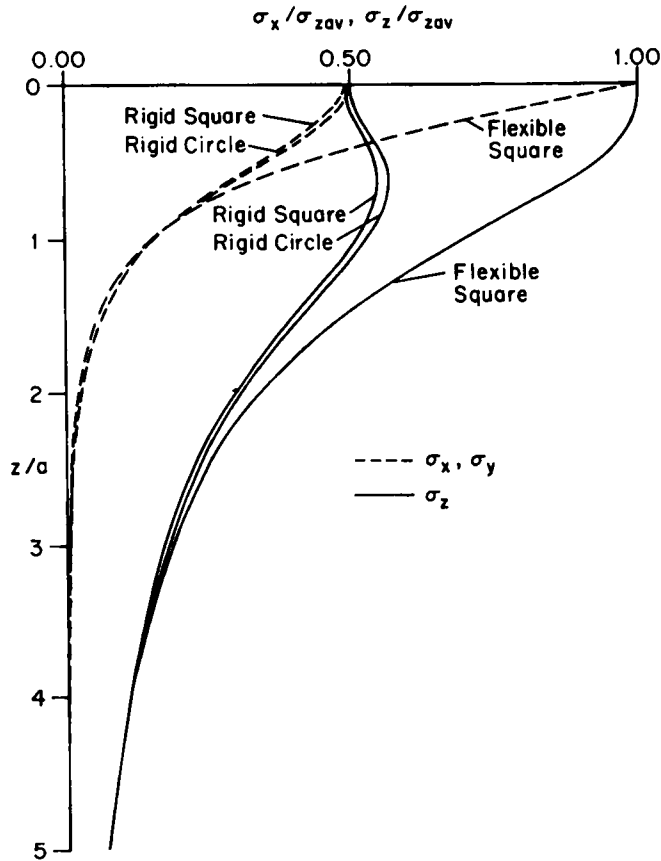


Figure 4. Normal stresses below the centroid of some smooth footings

between 0.5 and 0.333). The actual values presented in Figure 4 are for $\nu = 0.5$. All the curves at cutoff ($z/a = 5$) are within 2 per cent of σ_{zav} of the stresses from the Boussinesq solution.[‡]

The stress distributions for the flexible footing differ significantly from those of the rigid footing.[§] In contrast, the stress distributions from the rigid circular footing closely follow those of the rigid footing (within 2 per cent of σ_z/σ_{zav}), with the σ_z distributions for both possessing the near-surface peak typical of half-space response to rigid loading. Moreover the circular stresses exceed those of the rigid rectangle so that the results for the circle constitute a good conservative estimate of those for the rigid rectangle.

The second interior stress figure, Figure 5, shows the effect of varying the aspect ratio ($\alpha = 2, 5$) on the normal stresses beneath the centre of a rigid rectangular footing. Here σ_x no longer equals σ_y and curves for all three components are given. Again Poisson's ratio variations

[‡] The Boussinesq solution here gives the stresses within the half-space under an equivalent point load and may be obtained from, for example, Love.⁹ In all subsequent figures cutoff is at $z/a = 5$ and agreement with the corresponding Boussinesq solution is within 2 per cent.

[§] These differences are not significantly reduced if one compares the flexible footing with an average depth of penetration equal to the uniform depth of the rigid footing and sharing the same area (therefore having a different σ_{zav}).

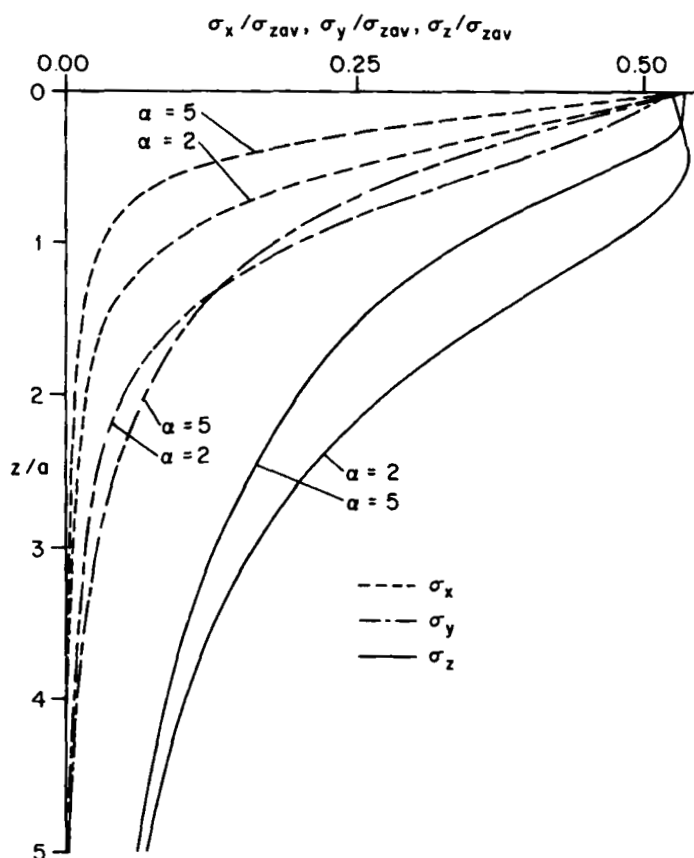


Figure 5. Normal stresses below the centroid of a smooth rectangular footing with varying aspect ratio (α)

are small, with the actual value being $\nu = 0.5$. Generally, increasing the aspect ratio, α , lowers the normal stress value and, in particular, reduces the peak or high values.

Interior stresses below the corner of a rigid square ($\alpha = 1$) footing are shown in the next figure, Figure 6, where values of σ_x/σ_{zav} ($=\sigma_y/\sigma_{zav}$) and σ_z/σ_{zav} are presented. For a comparison, stresses beneath a point on the circumference of the rigid circular footing and below the corner of the flexible square footing are both shown for the z -direction (again, all footings have the same area). Once again the variations obtained from a change in Poisson's ratio are small, with the actual value being $\nu = 0.5$. Now the stresses under the rigid circular footing differ by 13 per cent of σ_z/σ_{zav} but are still conservative. Both curves reflect the singularity that occurs as the edge of a rigid footing is approached ($z/a \rightarrow 0$). Although the singularity at the corner of the square footing is stronger than that at the edge of the circular, the cross-over—where the rectangular stresses start to exceed the circular—is so close to the surface as to be not discernable on the scale of Figure 6. In practical terms this means that the stresses in the region where the elastic estimates for the rectangular footing exceed those of the circular footing ($z/a \ll 1$) are sufficiently high so as to have probably induced yielding and a levelling off in their values: thus the elastic, circular footing, stresses in effect furnish an upper bound on the rectangular stresses for all z/a .

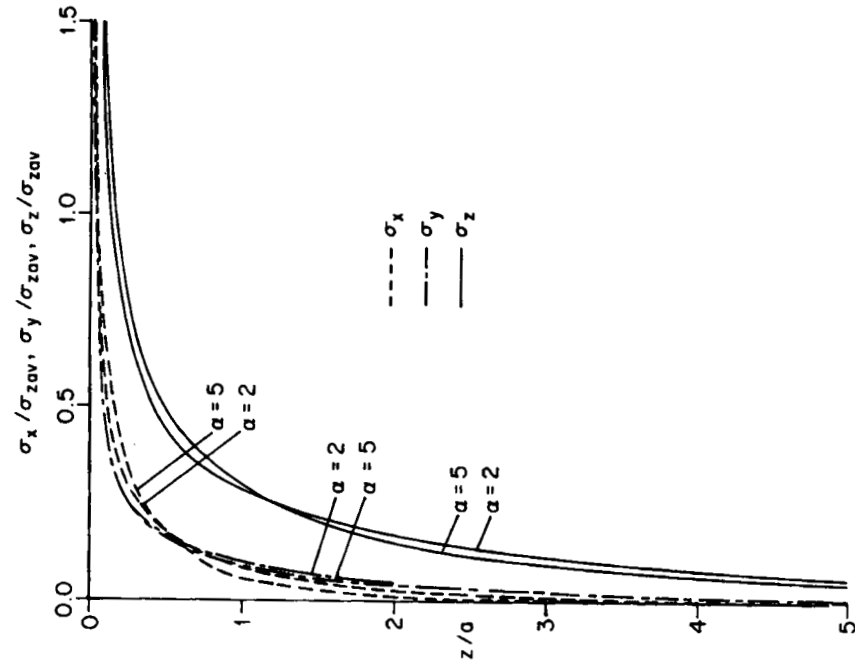


Figure 7. Normal stresses below the corner of a smooth rectangular footing with varying aspect ratio (α)

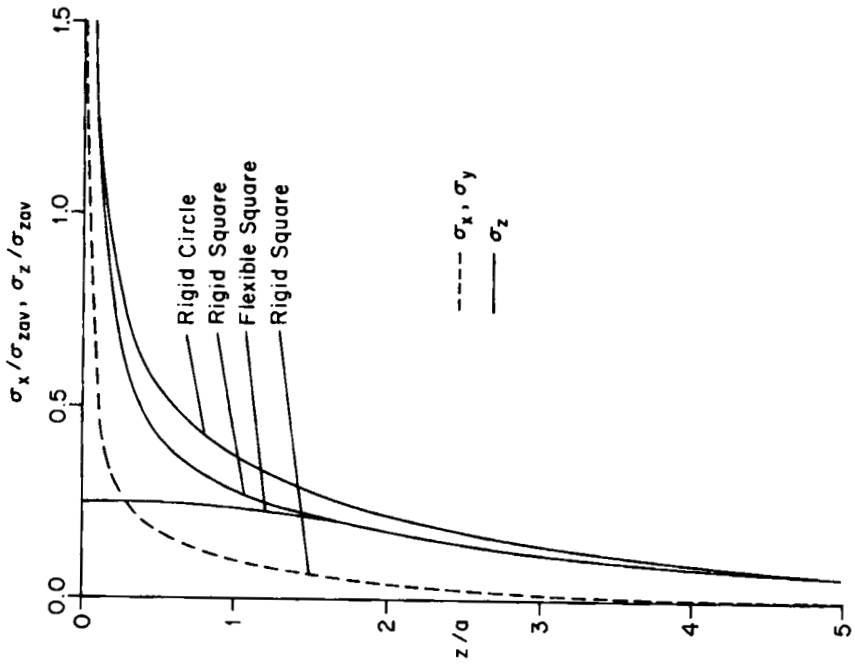


Figure 6. Normal stresses below the corner/edge of some smooth footings

The last set of curves, Figure 7, shows what effect varying the aspect ratio ($\alpha = 2, 5$) has on the normal stress components ($\sigma_x, \sigma_y, \sigma_z$) beneath the corner of the rigid rectangular footing. Here again Poisson's ratio variations are small, with the actual value being set to $\nu = 0.5$. Past some initial depth into the half-space, increasing the value of the aspect ratio decreases the value of the stresses in all three directions. The same singular behaviour of the stresses beneath the corner of the rigid rectangular footing that was observed in Figure 6 is also seen here.

REFERENCES

1. H. G. Poulos and E. H. Davis, *Elastic Solutions for Soil and Rock Mechanics*, Wiley, New York, 1974.
2. H. D. Conway and K. A. Farnham, 'The relationship between load and penetration for a rigid, flat-ended punch of arbitrary cross section', *Int. J. Engng* **6**, 489 (1968).
3. M. I. Gorbunov-Possadov and R. V. Serebrjanyi, 'Design of structures on elastic foundations', *Proc. Fifth Int. Conf. on Soil Mech. and Foundation Engng*, **1**, 643 (1961).
4. N. M. Borodachev and L. A. Galin, 'Contact problems for a stamp with narrow rectangular base', *Prikl. Mat. Mekh.* **38**, 108 (1974).
5. P. W. Brothers, G. B. Sinclair and C. M. Segedin, 'Uniform indentation of the elastic half-space by a rigid rectangular punch', *Int. J. Solids Struct.* **13**, 1059 (1977).
6. P. W. Brothers, *M.E. Thesis*, University of Auckland, New Zealand (1977).
7. I. N. Sneddon, 'Boussinesq's problem for a flat-ended cylinder', *Proc. Camb. Phil. Soc.* **42**, 19 (1946).
8. D. L. Holl, 'Stress transmission in earths', *Proc. High. Res. Board*, **20**, 709 (1940).
9. A. E. H. Love, *A Treatise on the Mathematical Theory of Elasticity*, Dover, New York, 1944.